3-D MEMS Based Real-Time Minimally Invasive Endoscopic Optical Coherence Tomography

Daniel T. McCormick[1,2], Woonggyu Jung[3,4], Veljko Milanović[2], Zhongping Chen[3,4] and Norman C. Tien[1,5]

[1]Berkeley Sensor and Actuator Center
Department of Electrical Engineering and Computer Science, University of California, Berkeley
[2] Adriatic Research Institute, Berkeley, CA 94706
[3]Beckman Laser Institute
[4]Department of Biomedical Engineering, University of California, Irvine
[5]Department of Electrical and Computer Engineering, University of California, Davis

A 3-dimensional, endoscopic optical coherence tomography (OCT) system based on a high-speed micromachined scanning mirror is presented. Cross sectional images of in-vitro and in-vivo samples are obtained and continuously displayed to the user. The optical resolution of the system is approximately 20μm×20μm×10μm. The endoscopic OCT probe has been utilized to identify cancerous regions of hamster cheek pouch tissue in real-time.

In this work we present an endoscopic OCT system based on a micromachined MEMS probe. The sampling resolution of each voxel is 10μm×10μm×10μm; the optical resolution is 20μm×20μm×10μm. In this study test-structures as well as *in-vitro* and *in-vivo* biological tissue samples have been imaged. Cross-sectional images are collected and displayed in real-time; these images may subsequently be combined to reconstruct a 3D image of the sample. Images from the 3D endoscopic MEMS OCT system have been utilized to clearly identify structures and features of tissue as well as the initial stages of cancer in hamster cheek pouch tissue by experts in the field.

Optical coherence tomography is an imaging modality capable of providing high resolution cross-sectional images of tissue and other materials.[1,2] A schematic diagram of the 3D MEMS OCT system is provided in Figure 1. Light from a low coherence source (1310nm, bandwidth of 70nm) is coupled into a fiber-optic Michelson interferometer. A rapid-scanning optical delay (RSOD) in the reference arm provides a variable optical path length utilizing a grating to separately control the phase and group delays; in the sample arm the endoscopic MEMS scanning probe directs a focused laser onto the sample surface. The light from the fiber is coupled into a ϕ 500μm focusing GRIN lens prior to the MEMS scanner.

The MEMS scanning actuator is a monolithic, single crystal silicon (SCS), 2-dimensional, gimbal-less, vertical comb-driven structure. The devices are designed and realized in a self-aligned DRIE fabrication process on SOI[3,4]; the actuator die has an area footprint of 2.6mm×3.3mm. The mirrors are fabricated in a separate SOI process and bonded to the actuator; allowing the actuator and mirror to be independently optimized. The apertures are metalized, low-inertia, SCS structures with a thinned mirror plate (2-5μm), thick stiffening trusses ($\tilde{2}$5μm) and a tall standoff pedestal ($\tilde{1}$20μm). Scanners with 800μm, 1mm, 1.2mm and 1.6mm mirror diameters have been realized. Images of scanners with bonded mirrors are presented in Fig. 2.

The device employed in this particular study utilized a 1.2mm mirror, and exhibited x and y-axis resonant frequencies greater than 1kHz. The scan angle of each axis is 20° (optical). The devices are packaged in an acrylic package, which provides mechanical rigidity and protection as well as the electrical connections for the MEMS device. In addition, the endoscopic package is designed to redirect the optical beam at a 90° angle and allow precise 3-axis optical alignment of the GRIN lens and the mirror. A schematic diagram and an image of a packaged device are shown in Fig. 3.

Prior to integration with the OCT system the mirrors are independently characterized utilizing optical feedback in order to allow accurate position control for both static and resonant scanning.

The axial (depth) resolution is determined by the coherence length of the light source, 10μm in this system. The axial (x and y-axis) resolution is defined by the spot size of the focused beam, which is limited by the optical components. With the current setup the axial resolution is approximately 20μm.

The nominal scan length in this work is 1mm for both lateral axes and 1.4mm for the axial axis. Individual cross sectional slices are combined to reconstruct a 3D image. Fig. 4 presents a series of 2D images from sequential sections of rabbit trachea; important structural and physiological components including the epithelium, glands, submucosa and cartilage are clearly visible. Fig. 5 shows a 3D solid reconstruction a section of rabbit trachea from different perspectives. Following reconstruction of the image numerous image processing and animation techniques may be applied to extract additional information or to automate analysis.

Tissue samples from the cheek pouches of hamsters in the initial stages of cancer development (dysplasia) were imaged and real-time identification of sub-millimeter regions of dysplasia was achieved, Fig. 6.

The realization of a small scale 3D OCT probe with high spatial resolution as well as rapid image acquisition rates has numerous applications in clinical medicine and research, including real-time, non-destructive optical biopsies.

Daniel T. McCormick- email: dmcc@eecs.berkeley.edu
497 Cory Hall, University of California, Berkeley, CA 94720

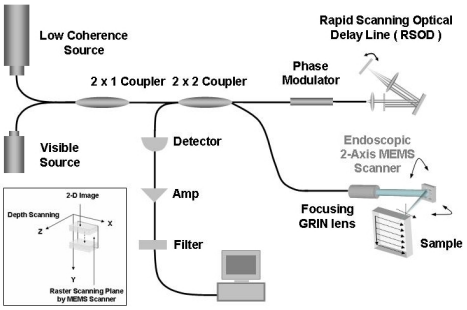

Figure 1. A schematic diagram 3-D MEMS based OCT system; the endoscopic MEMS probe is placed in the reference arm of the fiber-optic interferometer to provide high-speed 2-D scanning of tissue and other samples.

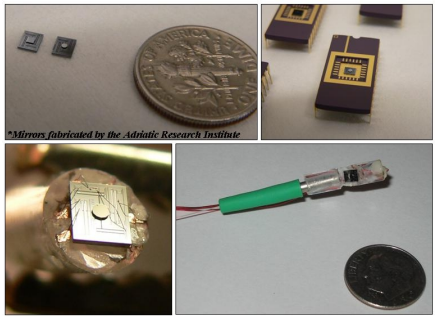

Figure 2. Optical images of: *(top left)* two 2.6mm × 3.3mm scanners with bonded mirrors, *(top right)* a device packaged in a standard DIP socket for bench-top characterization, *(bottom left)* a device attached and wirebonded to a probe assembly and *(bottom right)* a complete endoscopic probe with the MEMS scanner, GRIN lens, optical fiber and electrical connections.

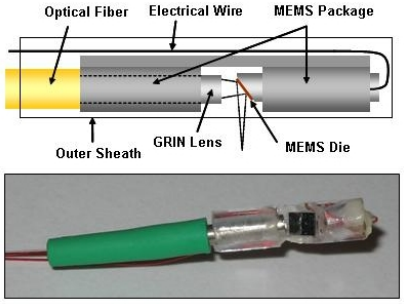

Figure 3. A schematic diagram of the endoscopic MEMS probe *(top)* showing the package, mirror and GRIN lens as well as the optical and electrical connections. An optical image of a packaged MEMS device *(bottom)*.

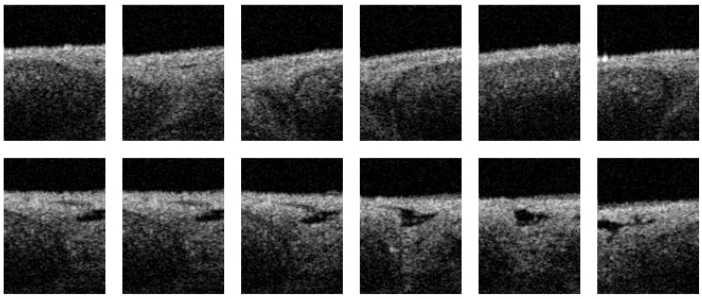

Figure 4. Two-dimensional OCT images taken from sequential 3D OCT scans in order to construct long lateral images; each image is 1mm×1.4mm with an optical resolution of 20μm×10μm.

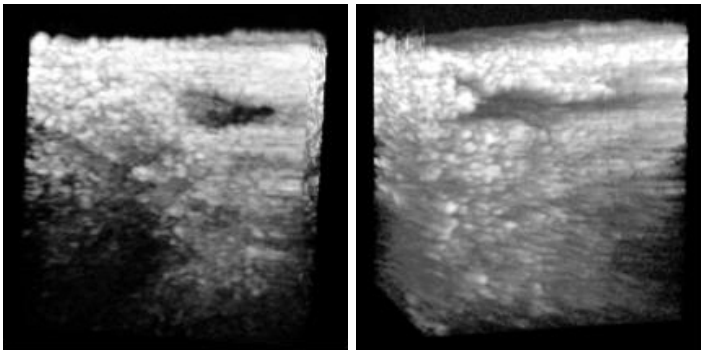

Figure 5. 3D OCT images of section of rabbit trachea, rotated in software to provide different perspectives; the images are 1mm×1mm×1.4mm and have an optical resolution of 20μm×20μm×10μm.

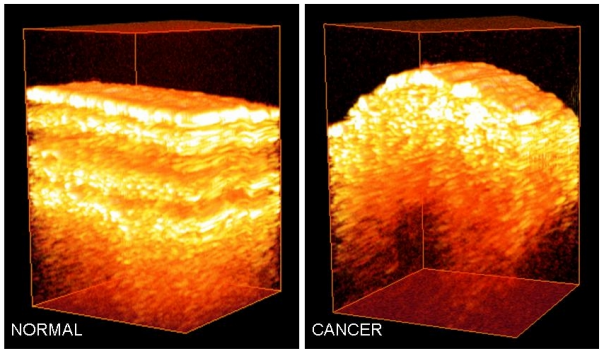

Figure 6. 3D images of *(left)* a section of normal hamster cheek pouch tissue and *(right)* a cancerous section of hamster cheek pouch tissue from the same animal. In the cancerous sample there is a clear lack of a basement membrane and visible layers; real-time identification of sub millimeter cancerous regions is achieved.

ACKNOWLEDGMENTS

This research is supported by grants from the NSF (BES 86924) and NIH (NCI-91717).

REFERENCES

1. D. Huang, E. Swanson, C. Lin, J. Schuman, W. Stinson, W. Chang, M. Hee, T. Flotte, K. Gregory, C. Puliafito, and J. Fujimoto, "Optical coherence tomography," *Science* **254**, pp. 1178–1181, 1991.
2. Y. Zhao, Z. Chen, C. Saxer, S. Xiang, and J. de Boer abd J.S. Nelson, "Phase-resolved optical coherence tomography and optical dopple r tomography for imaging blood flow in human skin with fast scanning speed and h igh velocity sensitivity," *Opt. Lett.* **25**, p. 114, 2000.
3. V. Milanonovic, "Multilevel-beam soi-mems fabrication and applications," *IEEE/ASME Journal of Microelectromechanical Systems* **13**, pp. 19–30, 2004.
4. V. Milanonovic, D. McCormick, and G. Matus, "Gimbal-less monolithic silicon actuators for tip-tilt-piston micromirror applications," *IEEE J. of Select Topics in Quantum Electronics* **10**, pp. 462–471, 2004.